COMPDYN 2015
5th ECCOMAS Thematic Conference on
Computational Methods in Structural Dynamics and Earthquake Engineering
M. Papadrakakis, V. Papadopoulos, V. Plevris (eds.)
Crete Island, Greece, 25–27 May 2015

STIFFNESS MODELING OF RC COLUMNS REINFORCED WITH PLAIN REBARS

Okan Ozcan[1]

[1] Akdeniz University, Department of Civil Engineering, 07058, Antalya, Turkey
e-mail: ookan@akdeniz.edu.tr

Keywords: Reinforced concrete; columns; effective stiffness; plain rebars; guidelines

Abstract. *Inaccurate predictions of effective stiffness for reinforced concrete (RC) columns having plain (undeformed) longitudinal rebars may lead to unsafe performance assessment and strengthening of existing deficient frames. Currently utilized effective stiffness models cover RC columns reinforced with deformed longitudinal rebars. A database of 47 RC columns (33 columns had continuous rebars and the remaining had spliced reinforcement) that were longitudinally reinforced with plain rebars was compiled from literature. The existing effective stiffness equations were found to overestimate the effective stiffness of columns with plain rebars for all levels of axial loads. A new approach that considers the contributions of flexure, shear and bond slip to column deflections prior to yielding was proposed. The new effective stiffness formulations were simplified without loss of generality for columns with and without lap-spliced plain rebars. In addition, the existing stiffness models for the columns with deformed rebars were improved while taking poor bond characteristics of plain rebars into account.*

1 INTRODUCTION

Effective stiffness predictions in performance based seismic assessment of existing structures primarily affect the dynamic characteristics of structures via structural demand estimations (lateral deformations and shear) and consequently the cost of seismic retrofit. In this respect, the strong dependence of effective stiffness on column axial load level was recognized by various researchers [1-8].

In addition, the influence of other parameters such as shear span to depth ratio, eccentricity and longitudinal reinforcement on effective stiffness was investigated and proposed stiffness formulations were modified accordingly [3, 5, and 9]. Moreover, simplified design implications were imposed in various structural guidelines [10-14] using the axial load level as the main design parameter. The literature study conducted on the effective stiffness reveals that all effective stiffness formulations are for columns longitudinally reinforced with deformed rebars. ASCE/SEI 41 update report [15] states that lower effective stiffness values might be attained for the structural components with plain rebars due to the reduced bond stress levels without further elaboration. Thus, it is expected that the effective stiffness recommended in assessment guidelines may show a tendency to overestimate the effective stiffness of vertical load bearing members having plain reinforcement. In addition, since the effective stiffness estimations substantially influence the anticipated seismic deformation demands, internal force distribution and dynamic response [3, 5, 7 and 8], special attention should be paid especially for the performance based assessment of structures reinforced with plain rebars. Therefore, the aim herein is to propose sound column effective stiffness estimations for columns having plain rebars.

2 COLUMN DATABASE

In order to examine the stiffness properties of RC columns with plain rebars, a database including 47 RC columns was formed [16] in which 33 of the columns were continuously reinforced and the remaining columns were spliced with various splice lengths. The database consisted of monotonic and cyclic lateral force – tip deflection responses of rectangular RC columns that were tested in single curvature. The axial load upper limit as taken from the database is 63% of the axial load carrying capacity with a shear span to depth ratio range of 2.8 to 9.2. In addition, longitudinal reinforcement ratios ranging between 0.6% and 2.5% were used with splice lengths from 15 to 40 bar diameters. The monitored failure mechanisms for the columns in the database were flexure dominant (i.e. longitudinal rebar yielding in tension accompanied by other limit states such as concrete crushing, rebar buckling and rebar fracture) in addition to lap-splice failures for inadequate splice lengths.

2.1 Spliced Steel Model

Instead of a constitutive steel model that was used for continuous rebars a spliced steel model was generated for plain rebars considering the failure mechanism as pull-out rather than splitting failure that is usually observed in columns with deformed reinforcing bars. For the spliced steel model, the strain decomposition method was implemented in which the total strain was assumed to be decomposed into elongation and slip components. The strain components were calculated iteratively while satisfying equilibrium and bond stress equations concurrently [16]. The adopted constitutive relationship of bond stress and slip depends on maximum bond stress and maximum slip [17]. Since the confining stresses primarily affect the bond stresses and corresponding slips for deformed reinforcement pertinent to splitting type of bond failure, the confining stresses were taken as zero as it would merely affect the bond behavior of plain rebars.

In addition, the maximum bond stress expression was modified for plain rebars using the lap-spliced beam database that was obtained from literature [18]. The splices were located at the bottom tension reinforcement with various splice lengths in the middle of the beams. Analytical calculations were based on standard section analysis carried out by the constitutive models of concrete [19] and spliced steel [16]. In the analyses, the analytically obtained beam moment capacities were compared with experimental moment capacities in order to acquire the maximum bond stress expression for plain rebars. Hereby, the maximum bond stress was determined as $\tau_{max} = 0.5\sqrt{f_c'}$ while providing the analytical to experimental moment capacity ratio close to unity.

2.2 Stiffness Approximations and Code Comparisons

The experimental effective stiffness calculations for the columns were based on estimated yield deflections ($\Delta_{y,exp}$) according to the yield forces (f_{fy}) that were determined by either standard section analysis (SSA) or load deflection curves due to the unavailability of the measured strain data for longitudinal reinforcement. Thus, the incipient yield deflections (Δ_{fy}) were determined initially as corresponding to the preceding lateral force (F_{fy}) at which the tensile reinforcement yielded or concrete compressive strain reached 0.002 by using standard section analysis with the constitutive models for concrete, steel and spliced steel. In accordance with Elwood and Eberhard [7], for the cases where the experimental lateral strength ($F_{max,exp}$) did not exceed the calculated yield force by a minimum 7%, the yield force was assumed as 80% of the experimental lateral strength concerning the influence of axial load and shear induced failure mechanisms.

The experimental yield deflections were acquired by extrapolating the attained incipient yield deflections in proportion to the ratio of the lateral force at which the strain at extreme concrete fiber reached 0.004 ($F_{0.004}$) to the incipient yield force (Eq. 1a). The yield curvatures (κ_y) were determined similarly (Eq. 1b). The experimental effective stiffness ($EI_{eff,exp}$) is defined in Eq. 2a assuming a linear curvature distribution over the column shear span (L) and the flexural stiffness (EI_{flex}) is calculated as shown in Eq. 2b.

$$\Delta_{y,exp} = \Delta_{fy} F_{0.004}/F_{fy} \tag{1a}$$

$$\kappa_y = \kappa_{fy} M_{0.004}/M_{fy} \tag{1b}$$

$$EI_{eff,exp} = F_{0.004} L^3/3\Delta_{y,exp} \tag{2a}$$

$$EI_{flex} = M_{fy}/\kappa_{fy} = M_{0.004}/\kappa_y \tag{2b}$$

11 columns out of the database were identified as not yielding while the experimental lateral strength was not monitored to exceed the calculated yield force at least by 7%. Herein, 2 beams and 7 columns were not identified to yield due to the relatively low shear span to depth ratio of 2.8 and high axial load ratio beyond 30% that introduced the effect of shear and axial load induced failure mechanisms, respectively. The remaining 2 columns (1 lap-spliced column and 1 column with relatively low axial load ratio of 12%) were observed to exceed the calculated yield force by approximately 5%. In reference to the measured effective stiffnesses for continuous and lap-spliced columns, the influences of key parameters ranging in investigation limits are presented in Figs. 1a - 1i.

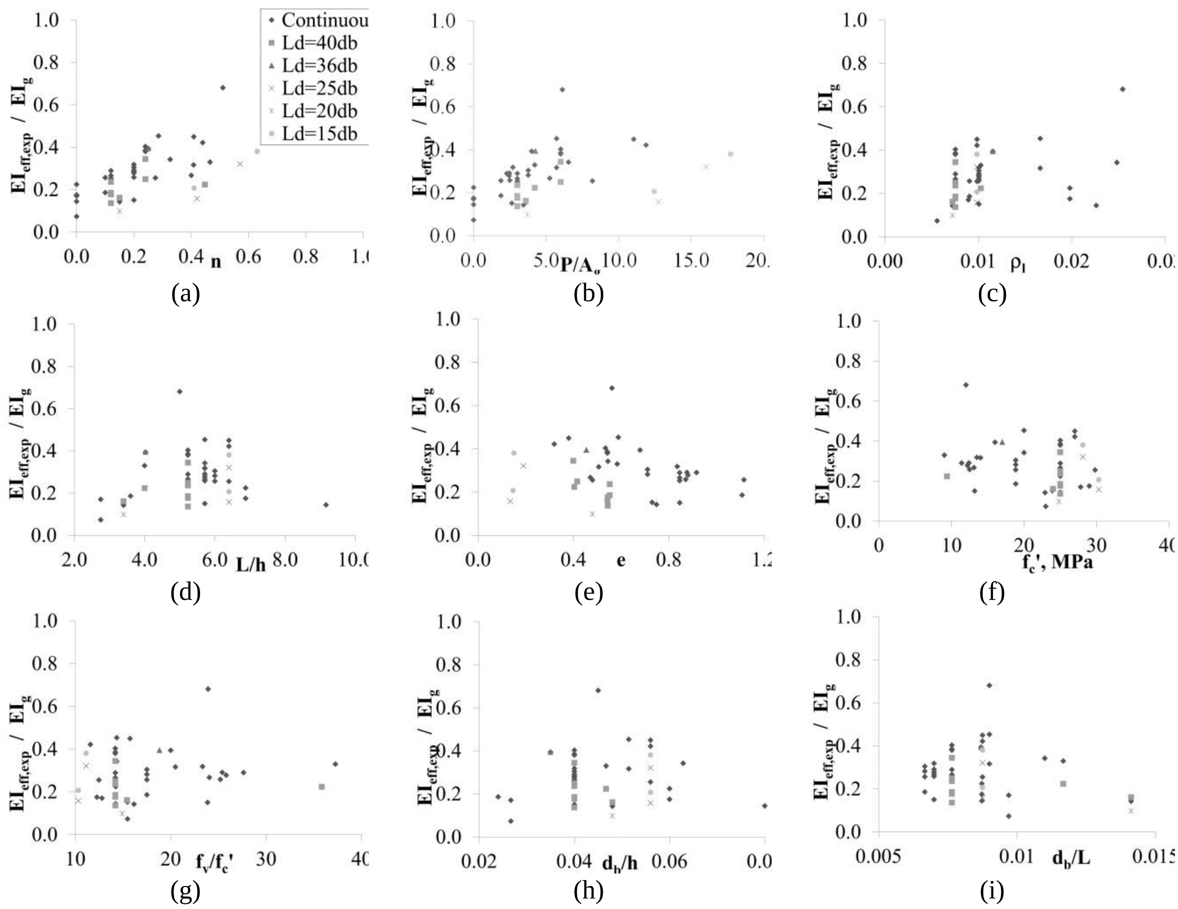

Figure 1 Experimental effective stiffness variations according to key parameters.

The most significant dependence can be observed for axial load level ($P/A_g f_c'$) in which P and $A_g$specify the axial load and gross cross-section area, respectively (Fig. 1a). However, due to the cluster of data below 7 MPa and increasing scatter beyond that region impeded the interpretation of the dependence of effective stiffness on mean axial stress (P/A_g) (Fig. 1b), additional tests to investigate the column performances beyond 7 MPa are needed for more reliable evaluation. Since the stiffening effect of axial compression on effective stiffness was verified among many researchers in the literature [3, 5-8], a similar response was observed for the columns longitudinally reinforced with plain rebars (Figs. 1a and 1b). The direct correlation between longitudinal reinforcement ratio (ρ_l) and effective stiffness can be attributed to the comparative increase in moment capacity rather than yield deflection with increasing reinforcement ratio (Fig. 1c) [5-8] however additional tests for longitudinal reinforcement ratios beyond 1% can provide better interpretation.

A slight influence of shear span to depth ratio (L/h) [6, 7 and 9] and eccentricity ratio ($e = M_{0.004}/Ph$) [5, 9] on the effective stiffness can be observed (Figs. 1d - 1e). Since the eccentricity ratio is infinite for the beams, the cases with no axial load were not included in Fig. 1e. The weakest interrelation with the column effective stiffness was examined for concrete compressive strength (f_c'), steel yield stress to concrete compressive strength ratio (f_y/f_c'), bar diameter to depth (d_b/h) and shear span ratios (d_b/L) as similar symptoms were attained in literature (Figs. 1f - 1i) [6, 7].

Guideline	**Expression (EI_{eff}/EI_g)**
ACI 318 [10]	$\begin{cases} 0.35, n < 0.1 \\ 0.70, n \geq 0.1 \end{cases}$
FEMA 356 [11]	$0.5 \leq n + 0.2 \leq 0.7$
ASCE 41 [12]	$0.3 \leq n + 0.2 \leq 0.7$
TEC-07 [13]	$0.4 \leq 4/3n + 0.8/3 \leq 0.8$
EC-8 [14]	$\frac{M_y L}{3EI_g\theta_y}, \theta_y = \frac{\kappa_y L}{3} + 0.013\left(1 + 1.5\frac{h}{L}\right) + 0.13\kappa_y \frac{d_b f_y}{\sqrt{f_c'}}$
Elwood and Eberhard [6]	$0.2 \leq 5/3n + 0.4/3 \leq 0.7$
Biskinis and Fardis [22]*	$a\left(0.8 + \ln\left(\max\left(\frac{L}{h}, 0.6\right)\right)\right)\left(1 + 0.048\min\left(50MPa, \frac{P}{A_g}\right)\right)$

* a is 0.081 for columns and 0.10 for beams.

Table 1 The guideline expressions for effective stiffness.

In line with the experimental data obtained from the column database, the stiffness approximations for columns with deformed rebars given in structural assessment guidelines (Table 1) were evaluated regarding the Figs. 2a and 2b. Since all guidelines predicted effective stiffness of the columns presuming deformed rebars as longitudinal reinforcement, a significant overestimation in effective stiffnesses was monitored for the columns longitudinally reinforced with plain rebars for all levels of axial load as shown in Fig. 2a. Herein, FEMA 356 [11] and TEC-07 (Turkish Earthquake Code – 2007) [13] gave the almost upper bound predictions of effective stiffness for low and high axial load ratios that represent the actual cases for beams and columns, respectively. For Eurocode 8 [14], the moments and curvatures at yield were computed according to the guideline provisions and compared with the aforementioned results of standard section analysis as shown in Figs. 3a - 3b. Herein, the overestimated yield moments were observed to have an increasing dispersion with the axial load as similar to the underestimated yield curvatures. Since the lower bond stress levels of plain rebars and poor bond slip performance enhanced the slip component of the yield deflections, the effective stiffnesses were monitored to be overestimated particularly for low axial load levels. However, for the columns under high axial load ratio, the development of slip induced deflections was not permitted as much as the columns under low axial load and the slip contribution can be expected to be higher for lap-spliced columns regarding the lower bond stress levels. The outcomes of the previous research [20-22] claimed the influence of poor bond performance of plain rebars on the yield deflection, yield strength and effective stiffness of RC columns to be insignificant considering a database including 20 columns reinforced with plain rebars.

Considering the inadequate bond strength along plain rebars that inhibited the full mobilization of yield strength, the yield moments were overestimated with an experimental to prediction ratio of 0.95 [20] and it can be anticipated that the development of yield strength can be inhibited further for lap-spliced columns as compared to the columns with continuous rebars. Thus, this phenomenon was found to be responsible for the reduced mean levels for yield moments (0.92 and 0.69 for continuous and lap-spliced, respectively) with a low scatter as shown in Fig. 3a. Further, the suggested empirical formulation by Biskinis and Fardis [22] (Table 1) was observed to underestimate the effective stiffnesses as compared to EC8-3 while satisfying slightly higher mean and standard deviation (Figs. 3c - 3d). However, the effective stiffness and yield properties of the columns should be evaluated while preventing shear force underestimations or displacement demand overestimations for low effective stiffnesses [7, 20].

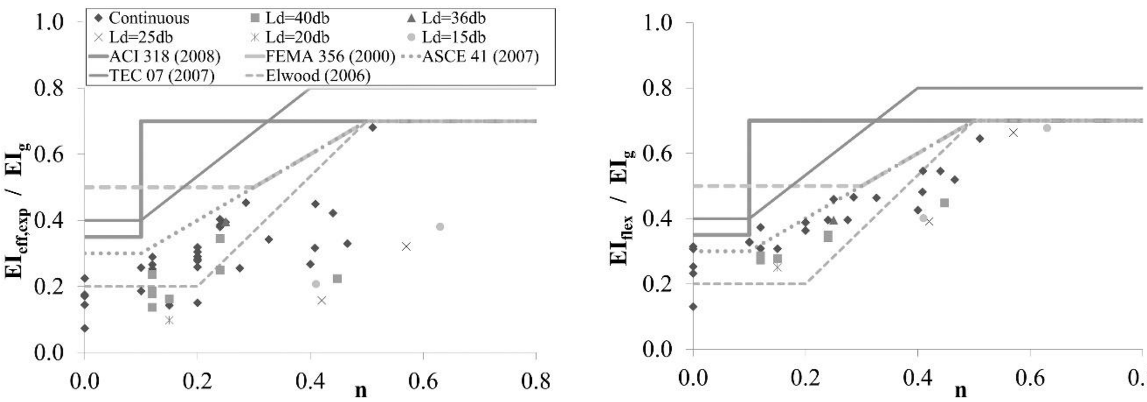

(a) (b)

Figure 2 The normalized (a) experimental effective stiffness and (b) flexural stiffness variations

The chord rotations at yield (θ_y) were computed accordingly with the components of flexure, shear and bond slip (Table 1) in order to determine the effective stiffnesses that were overestimated beyond axial load ratios of approximately 0.2 (Fig. 3c) while ignoring the effect of plain rebars. The closest and most reliable estimations were obtained by Elwood et al. [6] for low axial load levels up to the ratio of approximately 0.3, above which the effective stiffness was still overestimated. For all the investigated guidelines, effective stiffness overestimations can be attributed to the consideration of deformed rebars. Regarding the normalized flexural stiffness (EI_{flex}/EI_g), the most consistent predictions were obtained by ASCE 41 [12] and Elwood et al. [6] as shown in Fig. 2b. Since the other tip deflection contributors of shear and bond slip were not accounted, overestimations were majorly observed for the other guidelines (ACI 318, FEMA 356 and TEC-07) for all levels of axial load. Thus, the flexural stiffness estimations were reduced using the three component approach in order to provide more reliable predictions for the effective stiffness of the columns that were longitudinally reinforced with plain rebars.

3 EFFECTIVE STIFFNESS MODELING

The effective stiffness modeling estimations were based on the idea of reducing the flexural stiffness that was computed by standard section analysis pursuant to the adverse effects of shear and bond slip deformations. Since this phenomenon was a consequence of the three component approach in order to estimate column tip deflections, the same idea was utilized in effective stiffness computations for columns. The flexural component (Δ_{flex}) of the column yield deflection (Δ_y) (Eq. 3a) was computed as shown in Eq. 3b by integrating the curvature distribution which was assumed to be linear over the column shear span (L). Eq. 3c enables the calculation of the shear term (Δ_{shear}) of the yield deflection while being comparatively lower regarding the other sources of deformation such as flexure and bond slip. The effective shear area (A_v) and the effective shear modulus (G_{eff}) terms were concerned in order to reflect the deteriorating impact of shear cracking on column stiffness. Bond slip deflections (Δ_{slip}) were computed considering the rigid body rotation of the column as a result of elongation and slip of longitudinal rebars at the interface of column base and footing. Thereby, as shown in Eq. 3d, the bond slip component of yield deflection was calculated using the yield curvature (κ_y), rebar diameter (d_b) and column shear span (L). The bond strength for plain rebars was calculated by recalibrating maximum bond stress as ($\tau_{max} = 0.5\sqrt{f_c'}$). The experimental and analytical yield deflections are compared in Fig. 3e while providing close estimations except five lap-spliced columns for which the yield deflections were underestimated by a factor of 1.58 to 2.31.

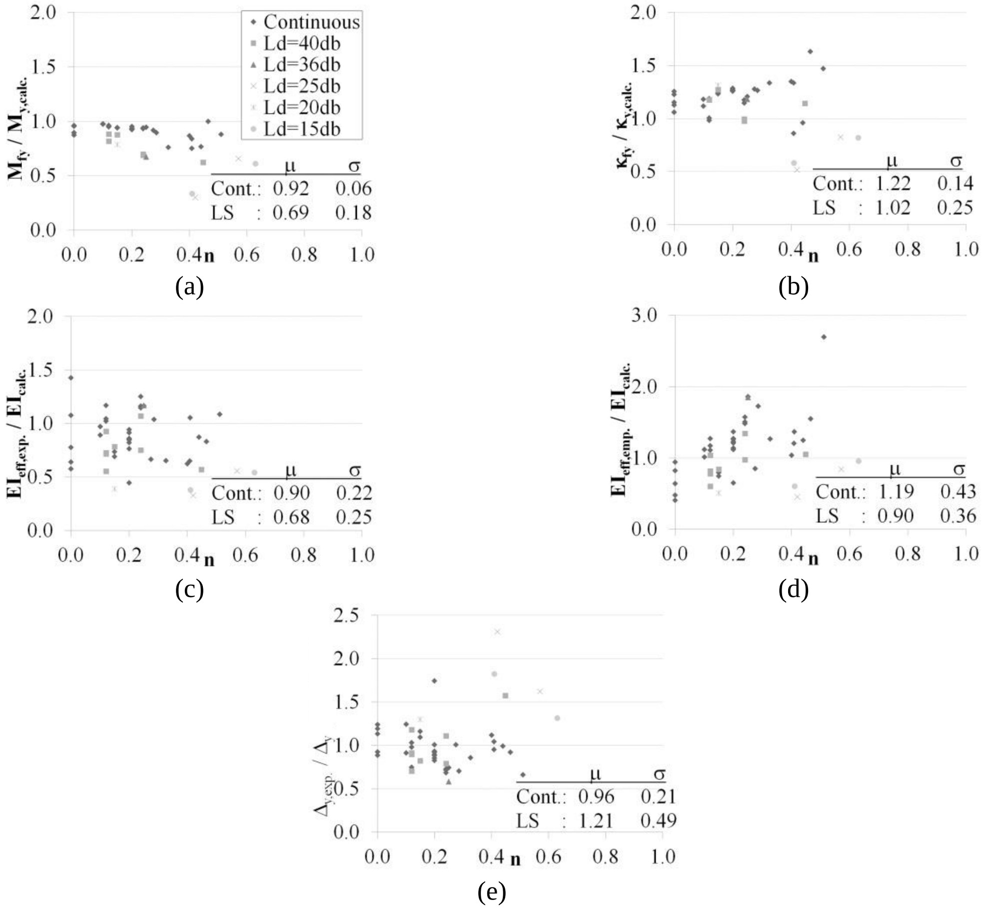

Figure 3 The comparison of experimental to calculated (a) yield moments, (b) yield curvatures, (c) effective stiffnesses according to Eurocode 8 (EC-8, 2005), (d) Biskinis and Fardis [22] and (e) yield deflections

$$\Delta_y = \Delta_{flex} + \Delta_{shear} + \Delta_{slip} \tag{3a}$$

$$\Delta_{flex} = \frac{\kappa_y L^2}{3} = \frac{M_{0.004}}{3EI_{flex}} \tag{3b}$$

$$\Delta_{shear} = \frac{M_{0.004}}{A_v G_{eff}} = \frac{4.8M_{0.004}}{A_v E_c} \tag{3c}$$

$$\Delta_{slip} = \kappa_y \frac{f_s d_b L}{8\tau_{max}} = \kappa_y \frac{d_b L}{4} \frac{f_y}{\sqrt{f_c'}} \frac{f_s}{f_y} \tag{3d}$$

Further, Eq. 2a was rewritten in terms of dimensionless parameters encapsulating Eq. 2b and Eqs. 3a - 3d that yielded Eq. 4 where $\alpha = EI_{flex}/EI_g$ denotes normalized flexural stiffness and $r_v^2 = I_g/A_g$ is the radius of gyration in loading direction. I_g and A_g denote the gross moment of inertia and gross cross-section area, respectively. The experimental and calculated effective stiffnesses are compared in Table 2.

$$\frac{EI_{eff,calc}}{EI_g} = \frac{\alpha}{1+17.28\alpha\left(\frac{r_v}{L}\right)^2+0.75\frac{f_s}{f_y}\frac{f_y}{\sqrt{f_c'}}\frac{d_b}{L}} \tag{4}$$

4 STIFFNESS MODELS

The aforementioned stiffness model acquired by Eq. 4 was further simplified in order to eliminate the need of standard section analysis. Considering design simplifications, the parameters of α and f_s/f_y were estimated in terms of only axial load (n) (Eqs. 5a - 5b) for continuous $(cont)$ columns as shown in Fig. 4. However, for lap-spliced columns, the parameters of splice length (L_d/d_b) and shear span to depth ratio (L/h) were embodied in addition to the axial load as presented in Eqs. 6a and 6b.

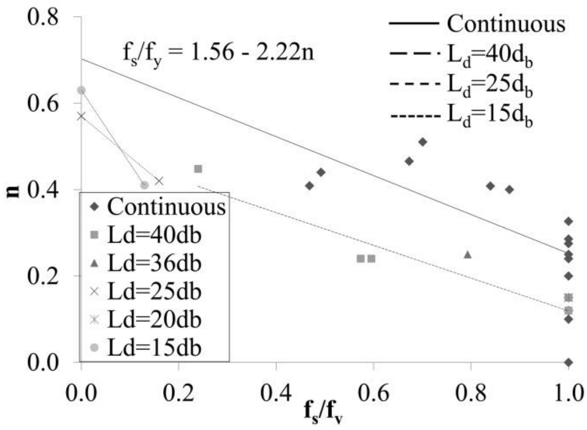

Figure 4 The variation of steel stress with axial load.

For Eqs. 6a - 6b, since the database did not include lap-spliced beams, the equations were valid within database limitations for axial loads in the range between 12 to 63% for lap-spliced columns and between 0 and 51% for the columns with longitudinal rebars. Table 2 demonstrates that reliable estimations could be obtained for the effective stiffnesses. As can be observed in Table 2, the introduced design formulations for continuous and lap-spliced columns had a good correlation with the analytical results. Furthermore, the predicted yield curvatures $(\kappa_{y,cont})$ [4] by Eq. 7a were monitored to correlate well with the continuously reinforced columns.

$$\alpha_{cont} = 0.26 + 0.65n \tag{5a}$$

$$\left(\frac{f_s}{f_y}\right)_{cont} = 1.56 - 2.22n \leq 1.0 \tag{5b}$$

$$\alpha_{LS} = 0.39n^{0.5}\left(\frac{L_d}{d_b}\right)^{0.05}\left(\frac{L}{h}\right)^{0.25} \tag{6a}$$

$$\left(\frac{f_s}{f_y}\right)_{LS} = 0.18n^{-1}\left(\frac{L_d}{d_b}\right)^{0.25}\left(\frac{L}{h}\right)^{-0.8} \leq 1.0 \tag{6b}$$

$$\kappa_{y,cont} = 2.1\frac{\varepsilon_y}{d} \tag{7a}$$

$$\kappa_{y,LS} = \kappa_{y,cont}\left(0.75n^{-0.06}\left(\frac{L_d}{d_b}\right)^{0.16}\left(\frac{L}{h}\right)^{-0.37}\right) = 1.575\left(\frac{\varepsilon_y}{d}\right)^{-0.06}\left(\frac{L_d}{d_b}\right)^{0.16}\left(\frac{L}{h}\right)^{-0.37} \tag{7b}$$

$$\frac{EI_{eff,calc}}{EI_g} = \frac{\alpha}{1+\beta\frac{d_b}{L}} \tag{8}$$

However, since this formulation tended to yield overestimated results for lap-spliced columns, Eq. 7a was modified for lap-spliced columns with regard to axial load, splice length and shear span to depth ratio (Eq. 7b). For the equations, ε_y and d identify the steel yield strain and column effective depth, respectively. In addition, Eq. 4 can be further simplified to yield Eq. 8 by ignoring the shear term in the denominator since it constitutes at most 3% of the tip deflection. In Eq. 8, α can be obtained by Eqs. 5a, 6a and the β constant has a value of 50 for plain reinforcement. Thus, Eq. 8 gave more realistic estimations (Table 2) as compared to the effective stiffness predictions of the previous studies that were related to the RC columns reinforced with deformed rebars [6, 7]. For the Eq. 8, the difference between two cases was ignored and a more general formula was suggested for the sake of simplicity.

Column Type	*	$\frac{EI_{eff,calc}}{EI_{eff,\exp}}$					$\frac{\Delta_{y,\exp}}{\Delta_y}$	$\frac{\alpha_{calc}}{\alpha_{pred}}$	$\frac{\kappa_{y,calc}}{\kappa_{y,pred}}$
		EC-8	a	b	c	d	e	f	g
Continuous (Cont.)	μ	0.90	1.19	1.08	1.04	1.02	0.96	0.97	1.02
	σ	0.22	0.43	0.21	0.25	0.26	0.21	0.12	0.11
Lap-Spliced (LS)	μ	0.68	0.90	0.95	0.91	0.98	1.21	1.06	1.02
	σ	0.25	0.36	0.36	0.35	0.32	0.49	0.12	0.09
Average	μ	0.83	1.10	1.04	1.00	1.01	1.04	1.00	1.02
	σ	0.25	0.43	0.27	0.28	0.28	0.33	0.13	0.10

* μ and σ: Mean and standard deviations for experimental to calculated ratios.
a. Biskinis and Fardis [22]
b. SSA: Standard section analysis
c. α, f_s/f_y : Cont: Eqs. 5a - 5b, LS: Eqs. 6a - 6b
d. α : Cont: Eq. 5a, LS: Eq. 6a, $\beta = 50$
e. Eq. 1a, Eq. 3a - 3d
f. Cont: Eq. 5a, LS: Eq. 6a
g. Cont: Eq. 7a, LS: Eq. 7b

Table 2 Mean and standard deviation variations.

Herein, the suggested values for $\alpha = 0.45 + 2.5\text{n}$ and $\beta = 110$ in literature [7] were shown to overestimate the effective stiffness of RC columns reinforced with plain rebars since the formulations were suggested primarily for RC columns with deformed rebars. In comparison with Eq. 5a, it can be inferred that the use of plain longitudinal rebars induced a lower rate of increase of flexural stiffness with axial load as compared to the deformed longitudinal rebars. All design formulations were compared in Table 2 and good estimations were provided since the terms of $\Delta_y, \alpha, \kappa_y$ could be predicted contiguous to experimental measurements. The recommended effective stiffness predictions for continuous columns were defined for upper and lower bounds for force based and displacement based analysis in case of either underestimating shear demands or overestimating displacement demands, respectively. Considering 90% of confidence level, the upper and lower bounds for effective stiffness were defined as shown in Eqs. 9a - 9c (Fig. 5a). For lap-spliced columns, the ratio of effective stiffness to gross stiffness was recommended to have a constant value of 0.2, since no significant trend was observed for varying splice lengths used in the database (Fig. 5b).

$$\left(\frac{EI_{eff}}{EI_g}\right)_{lowerbound} = 0.15 \leq \frac{1}{4}n + \frac{1}{8} \leq 0.25 \quad (9a)$$

$$\left(\frac{EI_{eff}}{EI_g}\right)_{mean} = 0.20 \leq \frac{5}{8}n + \frac{11}{80} \leq 0.45 \quad (9b)$$

$$\left(\frac{EI_{eff}}{EI_g}\right)_{upperbound} = 0.25 \leq n + \frac{3}{20} \leq 0.65 \quad (9c)$$

As a final remark, in common practice, the circular and rectangular cross sections generally pertain to RC bridge and building columns with low to high axial load level, respectively. Thus, circular columns are liable to possess lower axial load and d_b/L values with shear spans generally longer than ordinary building columns. Therefore, although all the formulations implemented in this research were based on a database of rectangular columns, the suggested formulations can also be utilized for circular columns regarding the range of variables under investigation.

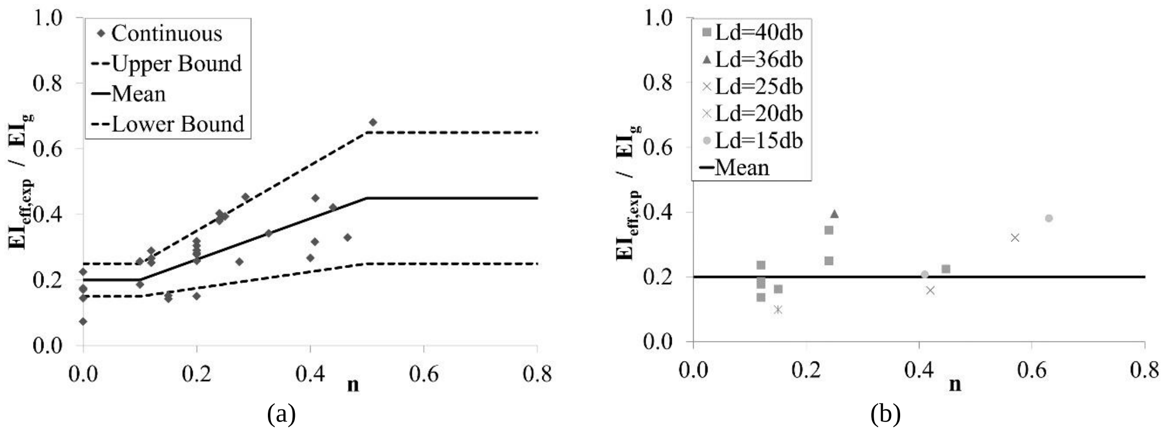

Figure 5 The effective stiffness recommendations for (a) cont. and (b) LS columns with plain rebars.

5 CONCLUSIONS

Predicting the effective stiffness for RC members is crucial in assessment and strengthening since the seismic characteristics and consequent response of RC structures is majorly influenced by cracking under gravity and lateral forces. The current guideline recommendations on effective stiffness of RC columns may mislead for plain reinforcement due to the major postulation of deformed rebars as longitudinal reinforcement. Thus, a RC column database was constituted by monotonic and reversed cyclic tests of 47 columns in which 33 columns were continuously reinforced and the remaining were spliced with various splice lengths. In the analysis of lap-spliced columns, the adopted spliced steel model from literature was modified using a lap-spliced beam database reflecting the failure mechanism of plain rebars. The analyses approved the dependence of effective stiffness on axial load and longitudinal reinforcement ratio as compatible with previous researches on deformed rebars. In this sense, it was ascertained that due to the shortcomings of the current structural guidelines upon utilization of longitudinal plain rebars, column effective stiffnesses were overestimated. Therefore, more reliable effective stiffness predictions were obtained by reducing the flexural stiffness of the columns regarding the deflection constituents of shear and bond slip on the basis of the three component approach while taking plain rebars into account. In addition, upper and lower bound effective stiffness expressions were recommended that can be utilized for force and displacement based assessment of RC structures, respectively.

REFERENCES

[1] Hage SE, MacGregor JG. *Second Order Analysis of RC Frames.*Univ. of Alberta; 1974.

[2] Paulay P, Priestley MJN. *Seismic Des. of RC and Masonry Buildings.* NY: J. Wiley; 1992.

[3] Mehanny SSF, Kuramoto H, Deierlein GG. Stiffness Modeling of RC Beam-Columns for Frame Analysis. *ACI Str. J.*; 98 (2): 215-25, 2001.

[4] Priestley MJN. *Myths and Fallacies in Earthq. Eng., Rev*. 9 M.Milne Lec.; Italy: 2003.

[5] Khuntia M, Ghosh SK. Flexural Stiffness of Reinforced Concrete Columns and Beams: Analytical Approach. *ACI Structural Journal*; 101 (3): 351-63, 2004.

[6] Elwood KJ, Eberhard MO. *Effective Stiffness of RC Columns*; Univ. of Calif., 2006.

[7] Elwood KJ, Eberhard MO. Effective Stiffness of Reinforced Concrete Columns. *ACI Structural Journal*; 106 (4): 476-83, 2009.

[8] Kumar R, Singh Y. Stiffness for RC Members for Seismic Analysis. *ACI Str.J.*; 107 (5): 607-15, 2010.

[9] Mirza SA., Flexural Stiffness of Rectangular RC Columns. *ACI Str.J*; 87(4): 425-35, 1990.

[10] ACI Committee 318. *Building Code Requirements for Structural Concrete and Commentary*. American Concrete Institute; Farmington Hills; MI: 2008.

[11] FEMA 356. *Prestandard and Commentary for Seismic Rehabilitation of Buildings*. *Federal Emergency Management Agency*; Washington; DC: 2000.

[12] ASCE 2007b. *Seismic Rehabilitation of Existing Buildings*, ASCE/SEI 41, Supplement I. American Society of Civil Engineers; Reston; VA: 2007.

[13] Turkish Earthquake Code (TEC). *Regulations on Structures Constructed in Disaster Regions*. Ministry of Public Works and Settlement; Ankara: 2007.

[14] European Committee for Standardization. *Design Provisions for Earthquake Resistance of Structures* EC-8; Brussels: 1994-2003.

[15] Elwood KJ, Matamoros A, Wallace JW, Lehman D, Heintz J, Mitchell A et al. Update to ASCE/SEI 41 Concrete Provisions. *Earthquake Spectra*; EERI; 23 (3): 493-523, 2007.

[16] Ozcan, O. Stiffness Modeling of RC Columns Reinforced with Plain Rebars, *Structural Engineering and Mechanics*, 50 (2), 163-180, 2014.

[17] Xiao Y, Ma R. Seismic Retrofit of RC Circular Columns using Prefabricated Composite Jacketing. *ASCE Journal of Structural Engineering*; 123 (10): 1357-64, 1997.

[18] Hassan MN. *Splice Tests of Plain Steel Bars in Concrete*. PhD Th.; Univ. of Sask.: 2011.

[19] Mander JB, Priestley MJN, Park R. Theoretical Stress-Strain Model for Confined Concrete. *Journal of Structural Engineering*; 114 (8): 1804-26, 1988.

[20] Fardis, M.N., Seismic Design, Assessment and Retrofitting of Concrete Buildings Based on EN-Eurocode8, Springer Geotechnical, Geological and Earthquake Eng., V8, 2009

[21] Fardis, M.N., Performance and displacement based seismic design and assessment of concrete structures in the model code 2010, *Struct. Concrete*, 14(3), 215-229, 2013

[22] Biskinis, D.E. and Fardis, M.N., "Deformations at flexural yielding of members with continuous or lap-spliced bars", *Struct. Concrete*, 11(3), 127-138, 2010.